Materials Science-Poland, 41(4), 2023, pp. 1-12
http://www.materialsscience.pwr.wroc.pl/
DOI: 10.2478/msp-2023-0043

Investigation of silver nanoparticles embedded in extracted gelatins from camel, bovine, and fish bones for possible use in radiation dosimetry

Thaar K. Alrashidi[1], Alwaleed Aljuhani[1], Faisal Almugaiteeb[2], Nacer Badi[1,*], Hatem A. Al-Aoh[3], Saleh A. Alghamdi[1], Abdulrhman M Alsharari[1], Ahmed Obaid M Alzahrani[4,5], Khaled Almalki[4,5]

[1]Department of Physics, Faculty of Science, University of Tabuk, 71491 Saudi Arabia
[2]King Abdulaziz Model Schools, Tabuk 47911, Saudi Arabia
[3]Department of Chemistry, Faculty of Science, University of Tabuk, Tabuk 71491, Saudi Arabia
[4]Physics Department, Faculty of Science, King Abdulaziz University, Jeddah, Saudi Arabia
[5]Center of Nanotechnology, King Abdulaziz University, Jeddah, Saudi Arabia

Gelatins from camel, bovine, and fish bones were successfully extracted by using chemical pretreatment and heating methods. The bones were demineralized for 3 days at ambient temperature using hydrochloric acid solutions (0.5–1 M), and the collagen was partially hydrolyzed by preheating in distilled water at 75–80°C for 3 h, followed by extraction temperature at 90°C for 1 h. Free-standing films of gelatin entrained with silver nanoparticles (Gel/AgNPs) at low concentrations (1.25, 2.5, and 5 mM) were synthesized as radiation dosimeters. A high-energy ultrasonic homogenizer was used to dissolve the gelatin in distilled water and to disperse the AgNPs in the gelatin. The nanocomposites' morphology and crystallinity were investigated using scanning electron microscopy (SEM), optical absorption, and Fourier transform infrared (FTIR) spectroscopies. Dose enhancement was assessed using X-ray irradiations with beam energies below and above silver K-edge. The beam was configured by setting the X-ray generator at 15, 25.5, and 35 kV potential and a beam current of 1 mA. An X-ray detector is used to detect the number of electrons after passing through Gel/AgNPs samples. The use of AgNPs embedded in gelatin caused the enhancement of X-ray radiation absorption, and the highest percentage of linearity for the dosimeter was found to be 90% in the optical range of 395 nm to 425 nm. The preliminary results demonstrated that Gel/AgNPs material may be used in radiation dosimetry for low-energy radiotherapy sources.

Keywords:

1. Introduction

Gelatin is a highly consumed protein in the pharmaceutical and food industries obtained through partial hydrolysis of collagen in animal bones, hides, and cartilage. Its uses in the food industry vary according to the product, as it controls product elasticity, texture, and emulsification. The most optimal method of producing high-quality gelatin is a significant consideration of pretreatment, temperature, and other extraction conditions [1]. Additionally, extracting gelatin from animals can help minimize the environmental hazards caused by wasting animal carcasses; for example, 19% of a camel's body is made of bones which are often not utilized, leading to a rise in waste levels and causing ecological damage. Gelatin is experiencing continuous growth, thus leading to increasing demand for acceptable, that is, halal/kosher, gelatin to populations of Islam and Judaism. Many of these religious adherents cannot consume porcine products. Subsequently, scientists have searched for substitutes for porcine gelatin over the last decade, which makes up approximately 46% of all gelatins [2]. Halal gelatins derived from bovine and fish sources are commercially available but camel gelatin is not. Each of these gelatins has its defining uses and characteristics. Camel gelatin is mainly a case of interest because it has not been commercially

* E-mail: nbadi@ut.edu.sa

produced yet, as it has the potential to avoid some of the other gelatin source's downsides, like allergen reactions that are usually caused by porcine and bovine gelatin, or even prove to have higher bloom levels (the measure of the gelatin's strength), than fish gelatin [3]. Gelatin can both absorb and scatter ionizing radiation due to its radiation-absorbing qualities. As a result, it has the potential to be a useful material for the creation of radiation-protective barriers or clothing for workers in radiation-risky settings. Although it only has a modest amount of X-ray attenuation and absorption on its own, it can be combined with other substances or altered to increase these properties. It may also be combined with pigments or dyes that change color when exposed to ionizing radiation. The amount of radiation exposure can be calculated by measuring the color change. Radiation dosimetry is the study of determining the most effective ionized radiation dose for radiotherapy while protecting healthy tissues near tumors. Various methods will achieve dependable radiation dosimetry [4]; however, gel dosimetry stands out in radiation oncology, as it can display a dose distribution that is highly appreciated qualitatively in three dimensions, which helps with establishing better treatment planning and better assurance with dose verification protocols [5]. The two main types of gel dosimeters, Fricke gel and polymer gel, vary according to their characteristics and applications. The polymer-gel dosimeter is based on radiation-induced polymerization and cross-linking of acrylic monomers, whereas the Fricke-infused gel dosimeter relies on radiation-induced oxidation of ferrous ions. Fricke gel dosimeters have the advantage of having excellent water and tissue equivalence for dosimetry [6–8]. However, due to the diffusion of ferric ions within the gel matrix, the primary drawback of these dosimetry systems is the loss of spatial information [9]. In radiation therapy for patients, polymer gel dosimeters are a promising radiation dosimetry technique [10]. Gel dosimetry has several benefits, such as tissue-like elemental composition, high spatial resolution, measuring doses in three dimensions (3D), and creating dosimeters with different sizes and geometries [11]. Polymer gels' ability to mimic tissue serves as a useful phantom for simulating the application of medical radiation to the human body. Recent research by De Deene [12] provided a thorough analysis of the historical advancements in gel dosimetry, with an emphasis on three key categories: (i) Fricke, (ii) radiochromic, and (ii) polymer gel dosimeters. In-depth reports on recent developments from these three groups are provided, along with individual viewpoints that concentrate on the ongoing difficulties high-performance dosimetry systems face. Additionally, Zhang et al. recently published a succinct review on hydrogel dosimeters for calculating ionizing radiation doses [13]. The work presented divides dosimetry into the following categories: (i) polymer hydrogels, (ii) Fricke hydrogel, (iii) radiochromic, (iv) radiofluorescent, and (v) NP-embedded dosimeters. These are highlighted for typical clinical applications, their key characteristics, and shortcomings. In particular, sensitivity, accuracy, and dose resolution are taken into consideration.

Gelatin has been widely applied in many medical fields (drug delivery systems and dosimetry) because of its stability post-radiation [14]. Although gelatin has a few downsides, like its relatively low melting point, which erases past data of dose distribution when melted, it has been used as a common dosimeter due to many factors like its near tissue equivalence, low cost, biocompatibility, and many other eco-friendly traits compared to other gel dosimeters [15]. In the medical field, specifically in ionized radiation therapy, gelatin is infused with metallic nanoparticles as opposed to bulk material due to nanoparticles' unique physiochemical characteristics. This allows them to enhance radiation sensitivity when infused with gels and make it easy to estimate doses using colorimetric readout methods [16, 17]. Other readout devices are based on radiation-induced processes and phenomena such as thermoluminescence (TLD) [18–20], optically stimulated luminescence (OSL) [20–23], electron spin resonance (ESR) [24, 25], and radioluminescence (RL) [26]. Dosimetry methods utilizing the aforementioned devices are well established in the available literature values for high-energy and high-dose irradiation in the number of

grays; however, dose registration in the sub-gray range is difficult.

Some examples of nanomaterials used in dosimetry are metallic nanoparticles of gold or platinum. However, the issue with such high atomic number nanoparticles is their price, for that reason silver nanoparticles (AgNPs), which are approved by the US Food and Drug Administration (FDA) in many medical applications, appear to be a good substitute because of their affordability [27, 28], and great dose enhancement of about 4 times when irradiated at a total absorbed dose of 12 Gy and 10 mM of silver nitrate solution [29]. The local dose enhancement is primarily made possible by secondary electrons produced by Ag re-emission. By identifying Ag K lines during radiation, it is possible to conduct remote monitoring and determine the spatial distribution of AgNP concentration. This information can be used to target tumors more effectively and increase local doses to better protect vulnerable organs nearby.

The aim of this work was to extract halal gelatin from camel, bovine, and fish bones using chemical pretreatment and heating techniques and then to form free-standing silver nanoparticle-enriched gelatin (Gel/AgNPs) films at room temperature. The samples were characterized for their potential use as dosimeters in low-energy radiotherapy sources. The inclusion of Ag nanoparticles into detector materials as additives could be a viable solution for increasing detector sensitivity and relatively high-photon absorption. Because of their large active surface area and relatively high photon-absorption ability, these nanoparticles can absorb a large amount of energy at lower irradiation levels, which is proportional to the absorbed dose.

2. Experimental

2.1. Chemical

The silver nanopowder with a purity of 99.99% and average size of 30–50 nm was purchased from US Research Nanomaterials, Inc., USA. Distilled water was used for the preparation of a silver colloidal solution-based gel dosimeter. Other chemicals used in processing the gel, such as hydrochloric acid and ammonium sulfate, were of analytical grade without further purification.

2.2. Gelatin extraction

2.2.1. Camel and bovine gelatin

Both camel and bovine gelatin were extracted by cutting the bones into approximately 3-cm pieces as shown in Figure 1a. The bones were cleaned of grease and impurities and boiled in water for two hours at a temperature of 90°C. After that, the bones were washed off and dried in the oven for 24 hours at 60°C. The bones were treated in 1M hydrochloric acid for 72 h at room temperature to demineralize and partially hydrolyze collagen (Fig. 1b). The remaining acid traces were removed by washing in cold water at less than 20°C. The bones were then neutralized using 4% w/v ammonium sulfate at 75°C for 3 h. The gelatin was extracted from the bones in distilled water in a ratio of 1:3 w/v at 90°C for 1 hour (Fig. 1c). The gelatin solution produced (Fig. 1d) was filtered through cheesecloth, and the supernatant was then vacuum dried at a temperature of 75°C for as long as necessary until all solvents evaporated, leaving a solid gel "gelatin," as shown in Figure 1e. Finally, the gel was then dried, ground into a powder (Fig. 1f), and stored at room temperature for later use.

2.2.2. Fish gelatin

Bones from tuna fish, which are depicted in Figure 2a as the main component of this study, were purchased from Lulu Hypermarket in Tabuk City (KSA). Fish bones were first thoroughly cleaned of meat and other impurities before being cut into smaller pieces, washed with tap water, and weighed. The fish bones (ossein) are then submerged in 0.5 M acidic solution at a 1:8 ratio for 48 hours (Fig. 2b). Next, they are washed in water with a pH of 5 to 6. After that, ossein was prepared for extraction by being put in a beaker and mixed with distilled water in a ratio of one to three. A temperature of 80°C was then applied for three hours of heating. This heating procedure uses a mixture of gelatin and bone byproducts that have been filtered using a filter cloth as shown in

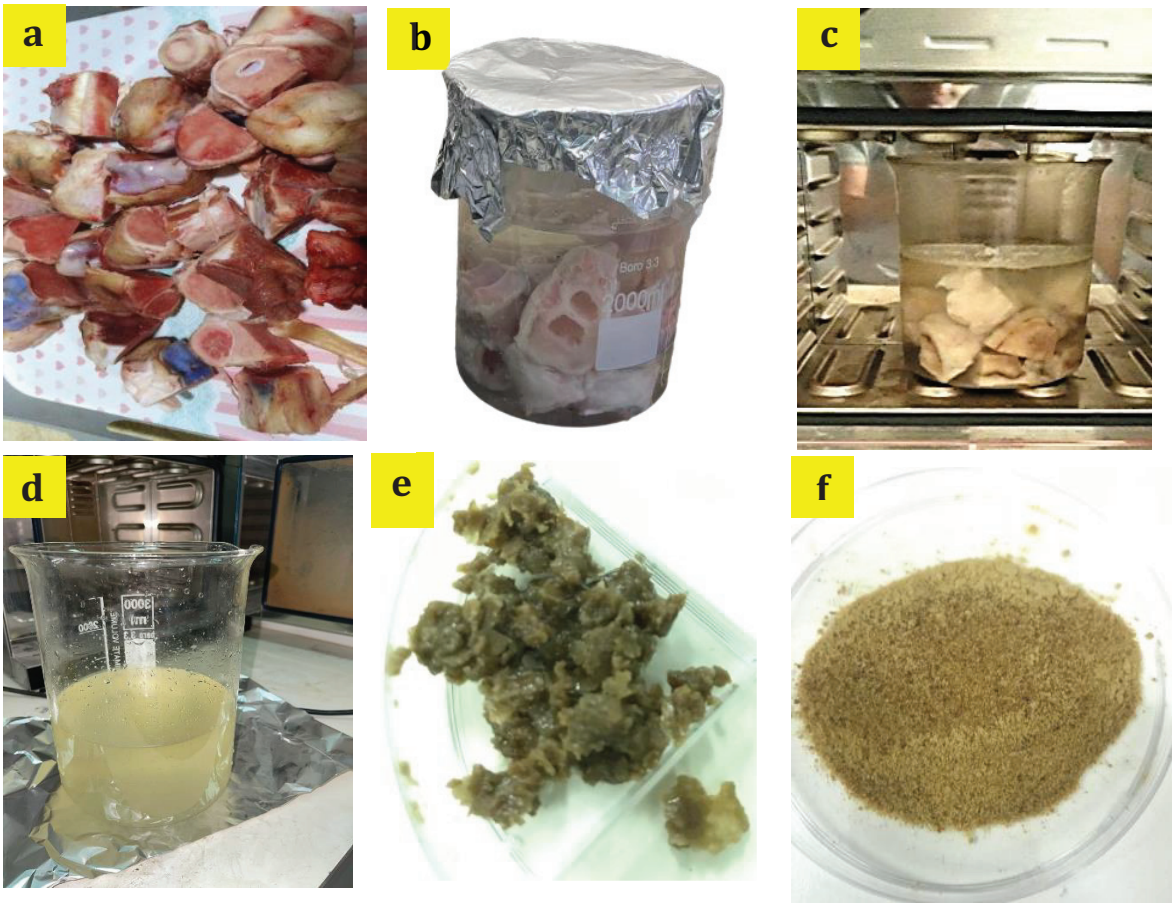

Fig. 1. Camel and bovine gelatin extraction process: (a) bone pieces, (b) demineralized and partially hydrolyzed collagen, (c) gelatin extraction, (d) filtered gelatin, (e) evaporation of solvent, (f) dried gelatin

Figure 2c. The gelatin solution produced was then vacuum dried at a temperature of 75°C (Fig. 2d) for as long as necessary until all solvent evaporated, leaving a solid gel "gelatin," as shown in Figure 2e. The gel was then dried, ground into a powder (Fig. 2f) and stored at room temperature for later use. The yield of gelatin produced was calculated by dividing the resulting dry weight of gelatin powder by the weight of the processed bones. Based on 1 kg of camel and bovine bones versus 0.45 kg of fish bones, the yield was approximately 5.1%, 5.8%, and 7.5%, respectively.

2.3. Preparation of gel dosimeter

To ensure the highest level of reproducibility in the preparation of the Gel/AgNPs, the samples were created on a benchtop in a fume hood with normal atmospheric conditions. Aqueous gelatin (30% by weight) silver colloidal solutions at low concentrations (1.25, 2.5, and 5 mM) were prepared in distilled water at room temperature. Free-standing films of gelatin entrained with silver nanoparticles (Gel/AgNPs) were synthesized as radiation dosimeters. In our case, thin films for dosimetry applications do not refer to the types of films commonly used in dosimetry, such as radiographic films also called X-ray film [30], which require chemical development, and radiochromic films, which are mainly used for 2D dose verification. After self-development, the latter is used to test and characterize X-ray devices such as CT scanners and radiotherapy linear accelerators (LINACs). Instead, our dose gelatin films are suitable as a human tissue equivalent for radiotherapy diagnosis and treatment. In this direction, other

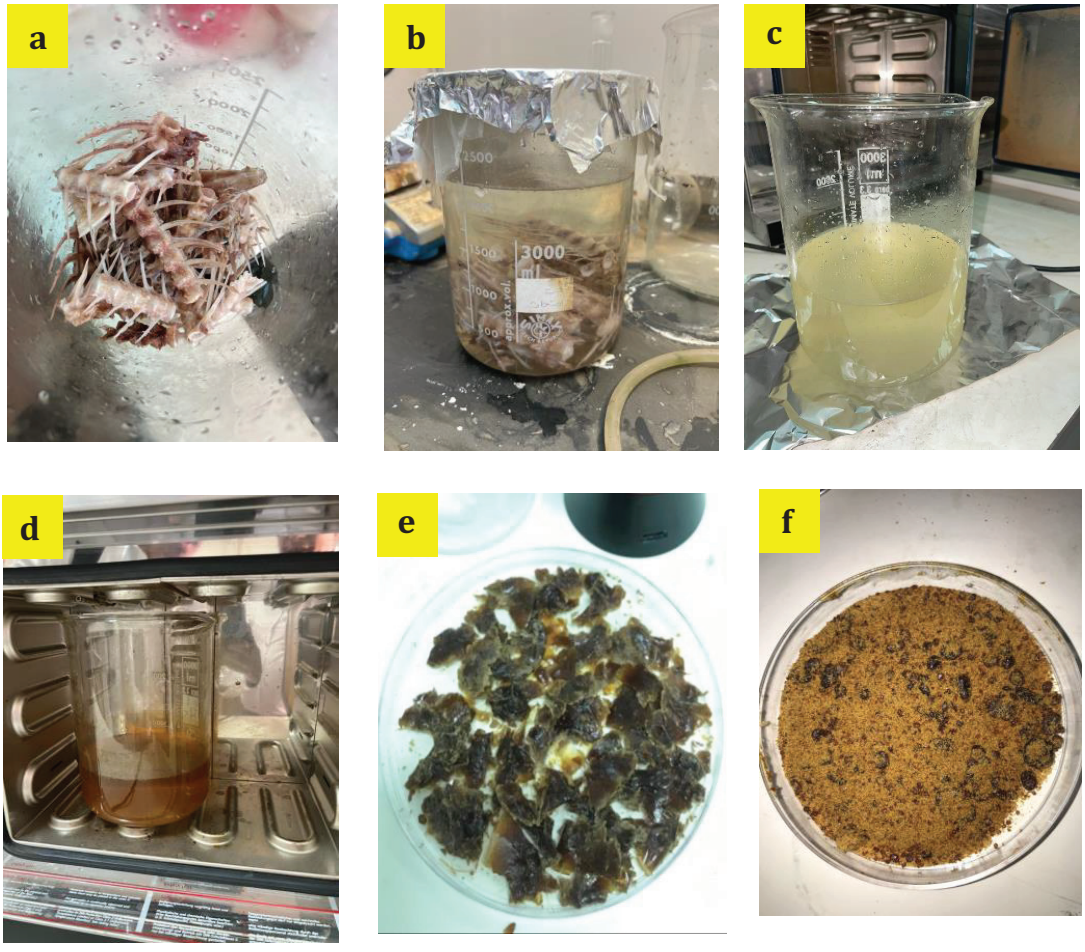

Fig. 2. Fish gelatin extraction process: (a) bone pieces, (b) demineralized and partially hydrolyzed collagen, (c) gelatin extraction, (d) filtered gelatin, (e) evaporation of solvent, and (f) dried gelatin powder

emerging polymeric materials may find application as ionization dose sensors. These include polar organic polymers such as polyvinyl alcohol (PVA) that contain salts of rare earth elements like gadolinium chloride ($GdCl_3$). When such composites are exposed to radiation doses, their optical properties change [31, 32]. PVA doped with 1 wt% Ni, NiO, and Fe_2O_3 nanoparticles was prepared and irradiated for radiation protection. PVA samples containing 1% Ni showed the highest mass attenuation coefficient values [33]. Cu/Zn reinforced polymer composites that had been exposed to alpha, proton, neutron, and gamma radiation and are more suitable for neutron shielding [34]. Gamma-ray attenuation parameters have also been studied in matrix composites such as high-density polyethylene doped with bismuth oxide nanopowders and polymer composites with $BaTiO_3$ and $CaWO_4$ [35, 36]. A polymer fiber Bragg grating (PFBG) was irradiated with fast neutrons at different doses from 24 to 720 Gy. Transmission and reflection studies have shown that PFBGs with high Bragg wavelengths are good candidates for use in dosimetry systems [37].

A 450 W U.S. solid ultrasonic homogenizer (Cleveland, USA) was used to dissolve and disperse the AgNPs in gelatin. The power of the ultrasonic homogenizer was kept between 30% and 100% of the maximum power of 450 Watts for up to 10 minutes of mixing time. These mixtures were then pipetted into a 30-mm glass dish and allowed to form transparent gels at room temperature where

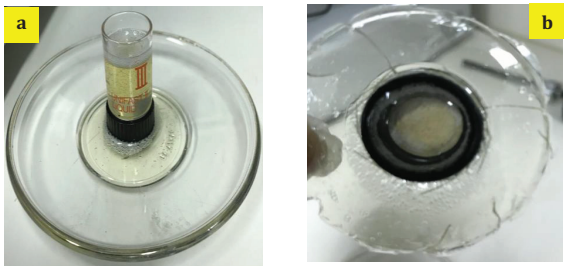

Fig. 3. Poured gelatin/AgNPs mixture (a) and peeled off film (b)

the slippery surface of the glass makes it easy to peel off the gel mixture. The thickness of the free-standing film was controlled by the amount of mixture poured into the glass dish as shown in Figure 3. The black round part in the center was used to lift the Gel/AgNPs films after they had solidified. Only a 1-mm thickness was required for this study of free-standing membranes. It is very difficult to control the thickness of raw gelatin in a research laboratory setup. In most published works, silver nanoparticles are introduced into a gelatin solution, which is poured into a vial of a certain thickness. The rheological properties of gelatin films are strongly influenced by and depend on the viscoelasticity, viscosity, and processing temperature of the film. The well-known process of producing gelatin in sheet or leaf form requires expensive equipment and is very time-consuming. This method of obtaining a gelatin film, especially a gelatin sheet, from powdered gelatin includes the following steps: plasticizing the powdered gelatin to which water is added by applying a shearing force at elevated pressure and elevated temperature; the softened fabric is extruded as a film through a slit die, the film is drawn from the slit, stretched, and the stretched film is dried. In this case, a large amount of air is drawn into the solution, so after the gelatin is completely dissolved, the air must be evacuated in a degassing apparatus to obtain a final product free of air bubbles.

2.4. Sample characterization

The morphology and crystallinity of the nanocomposites were investigated by using Philips XL 30 ESEM scanning electron microscope on an Au substrate, optical absorption, and Fourier-transform infrared spectroscopy (FTIR). The dose enhancement was assessed by using X-ray irradiations having beam energies below and above the silver K-edge, which is about 25.5 keV. The term "K-edge" describes the sharp increase in X-ray photon photoelectric absorption that is seen at an energy level just above the binding energy of the atom's k-shell electrons. The beam was configured by setting the X-ray apparatus (Leybold® 554-800) at 15, 25.5, and 35 kV potential and a beam current of 1 mA. An X-ray detector is used to detect the number of electrons in the air and after passing through Gel/AgNPs samples with a 2×2 cm^2 field size and a collimator to sample distance of 10 cm. The characterization of the free-standing film dosimeters was also carried out at room temperature by means of UV-visible absorption spectroscopy using Jenway 6800 Double-Beam (2-nm slit width) and ATR-FTIR (4000–225 cm^{-1}) spectrometers. The spectrometers were calibrated daily using the machines' "AutoCalibrate"? air calibration.

3. Results and discussions

3.1. SEM micrographs

Figure 4 shows a typical SEM micrograph of fish gelatin loaded with 1.25 mM silver nanoparticles. The highly conductive AgNPs are highly reflective under electron bombardment. They are not highly dispersive under ultrasonic mixing, and they tend to show some degree of agglomeration

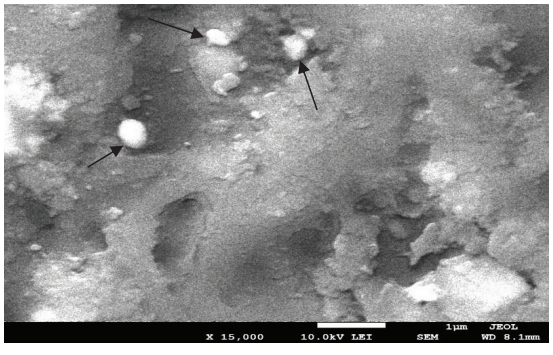

Fig. 4. SEM micrograph of fish gelatin mixed with 1.25 mM silver nanoparticles

and aggregation as indicated by the arrows, leading to the formation of submicron-sized silver particle clusters ranging from 150 to 250 nm, which negatively impacts the final product. The viscosity of the gel solution during processing affects the degree of agglomeration of infused nanoparticles. Therefore, decreasing the binder "gelatin" viscosity will certainly lower the formation of agglomerates. Agglomerates can be disrupted by sonication techniques to a certain degree, but aggregates cannot [38]. The addition of a surfactant, biological in particular, in this case may be needed to prevent both agglomeration and aggregation. It is stated in the sample preparation section above that once the gelatin has completely dissolved, a significant amount of air is drawn into the solution. The air bubbles have an obvious impact on mixing, and it is believed to give rise to agglomeration to some extent. We believe that if mixing is performed under vacuum for a reduction of air pockets, highly dispersed nanoparticles may be achieved.

3.2. FTIR Spectrum

Figure 5 shows the FTIR spectrum of a typically extracted fish gelatin in the form of a free-standing film. The obtained FTIR spectrum reveals that the peaks of gelatin transmittance are consistent with those reported in the literature [39–45].

FTIR measurements were performed to identify the possible biomolecules and bonds responsible for the structural and functional stability of fish bone-derived gelatin. Proteins are made up of amino acids linked by amide bonds. Peptide and protein repeat units give rise to nine characteristic infrared (IR) absorption bands, namely amides A, B, and I-VII [46]. Amide bands represent different vibrational modes of the peptide bond. The absorption band of gelatin in the infrared spectrum is in the region of the amide band; amide-I represents the C=O stretching/hydrogen bond coupling with COO, amide-II represents the bending vibration of the N-H group and the stretching vibration of the C-N group, and amide-III represents the coupling. The plane vibrations of the C-N and N-H groups of amides are coupled [47]. The peaks of the gelatin at 3305 cm^{-1} attributed to the presence of hydrogen bond water and amide-A, 1632 cm^{-1} peaks correspond to the occurrence of amide-I, a peak at 1542 cm^{-1} is indicating amide-II, a band at 1241 cm^{-1} indicates the amide-III, and peak ranges from 1445 cm^{-1} to 1335 cm^{-1} were attributed to the symmetric and asymmetric bending vibrations of the methyl group. The FTIR spectra of extracted gelatin from camel and bovine bones, which are not presented, show very similar typical transmittance peaks that correspond to the respective nine characteristic IR absorption bands.

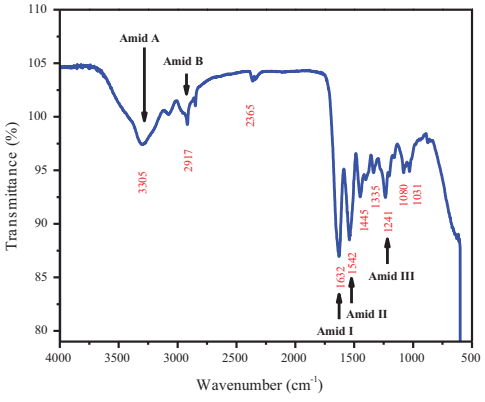

Fig. 5. FTIR spectrum of extracted fish gelatin

3.3. Optical absorption

Figure 6 shows the optical absorption spectrum of a 1-mm thick free-standing film made of

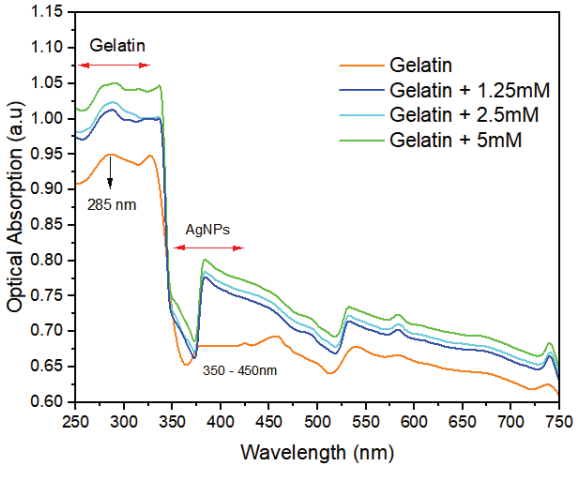

Fig. 6. Optical absorption spectra of extracted fish gelatin/AgNPs

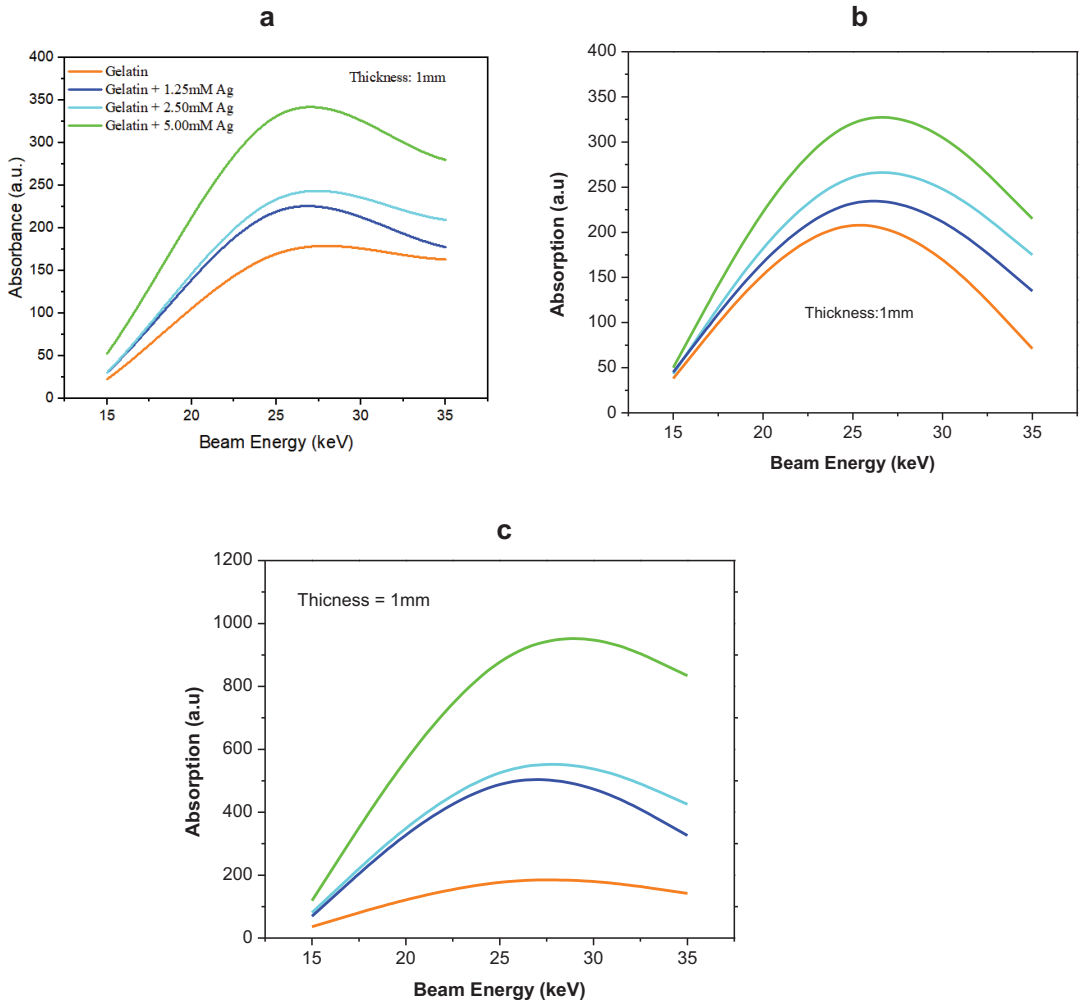

Fig. 7. X-ray absorption of a free-standing camel (a), fish (b), and bovine (c) gelatin/AgNPs

AgNP-entrained fish gelatin. As a result of surface plasmon resonance, silver nanoparticles are known to exhibit maximum optical absorption in the 350 nm–450 nm range depending on the size and shape of the nanoparticle [48]. In our case, the peaks are centered in the 395 nm–400 nm range, where pure gelatin exhibits relatively low absorption. As the amount of silver nanoparticles added to gelatin increases, however, the optical absorption of the mixture increases. The use of AgNPs embedded in gelatin caused the enhancement of X-ray radiation absorption and the highest percentage of linearity for the dosimeter is found to be 90% in the optical range of 385 nm to 425 nm. The camel and bovine gelatin samples tested showed qualitatively similar behavior, but slightly different amounts of optical absorption were recorded. In order to monitor the radiation dose in the synthesized nanocomposites, silver colloidal concentration is considered a good strategy in light of the works referred above [31–36].

3.4. X-ray absorption

Figure 7 shows the X-ray absorption of free-standing films made of AgNPs entrained camel (a), fish (b), and bovine (c) gelatin. The thickness of the films was 1 mm each and the potential was set to 15, 25.5, and 35 kV potential with a beam current of 1 mA. When exposed to 25.5 kV, silver nanoparticles exhibit their highest level of absorbance, indicating that the photon's energy is just slightly

higher than the silver nanoparticles' K-edge binding energy. Additionally, there is a direct correlation between the absorption and the amount of gelatin and silver nanoparticles. Tested samples showed qualitatively similar behavior, but different amounts of X-ray absorption were recorded. Bovine gelatin/AgNPs demonstrated the highest absorption, followed by camel and fish gelatin.

The attenuation coefficient μ which describes how easily the X-ray beam can penetrate a volume of the gelatin/AgNPs. It measures the total loss of the beam intensity, including scattering. It is estimated by using the Beer-Lambert law:

$$I = I_o e^{-\mu x} \quad \text{and} \quad \mu = \frac{\ln\left(\frac{I_o}{I}\right)}{x}$$

Where I_o is the incident X-ray beam intensity, I is the intensity of the collected passing beam through the gelatin/AgNPs sample, and x is the thickness of the sample.

Figure 8 shows the variation of μ with respect to the beam's energy. As expected, μ decreases as the energy of the X-ray source increases. The highest value of μ is found to be the one corresponding to the highest amount of infused silver nanoparticles in gelatin.

The absorbance of X-rays at three different discrete energies is shown as a continuous curve showing a maximum at about 25 keV, but the absorption coefficient shows a continuous decrease with beam energy. The absorption coefficient is defined as the rate at which the absorption is taking place, this

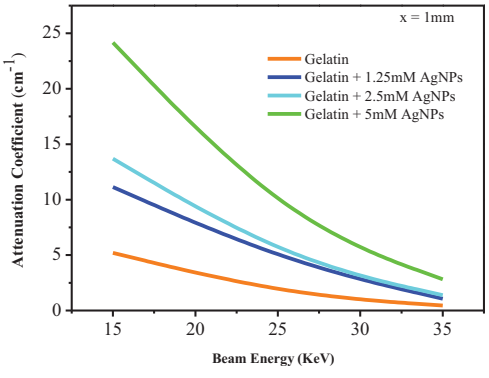

Fig. 8. Attenuation coefficient versus beam energy of a free-standing bovine gelatin/AgNPs

entity measures how quickly the X-ray beam would lose dose due to absorption alone while the attenuation coefficient μ describes how easily the X-ray beam can penetrate a volume of the gelatin/AgNPs. This corresponds to the rate at which the beam attenuates, or loses intensity, at depth. Because it measures the total loss of the beam intensity, including scattering, however, it can serve as a qualitative or a quantitative measurement entity depending on how strong or weak scattering tissue is. In short, this is because attenuation is a continuous energy loss, while absorption is a sudden energy loss when the X-ray beam encounters an absorbing object. The attenuation coefficient varies with the type of material and the energy of the radiation. In general, for electromagnetic radiation, the higher the energy of the incident photons and the less dense the material, the lower the corresponding attenuation coefficient [49]. The increase in loading silver nanoparticles in gelatin may also have caused the density of the nanocomposite to increase, leading to relatively higher values of the attenuation coefficient.

This preliminary finding shows that the free-standing films prepared using gelatin/AgNPs can be recommended as reliable materials for the fabrication of radiation dosimetry devices for low-energy external radiotherapy sources. The challenge in preparing high-sensitive, reliable 3D or 2D dosimeters is related mainly to sensitivity, precision, reproducibility, accuracy, resolution, and time for measurement, independent of the radiation quality of the final dosimeter. The three main steps of gel dosimetry are the following: (1) the radiation-sensitive gel solution is made and placed into a container, phantoms, and associated vials for calibration, (2) irradiation and polymerization of the gel solution, and (3) scanning of the polymerized gel by an appropriate imaging technique and subsequent analysis of acquired images. The second step—gel dosimetry—will be to expose the free-standing Gel/AgNPs composites to X-ray radiation. No solution and no polymerization are needed. However, aiming at step 3 necessitates exposing the free-standing Gel/AgNP films to high doses of x-ray radiation which can be controlled by the current beam value and exposure duration

while setting the beam energies below and above the silver K-edge. Using an X-ray generator with a high beam current of 10 mA which is ten times the beam setting that is currently in use will certainly result in a high dose. This anticipated work will lead to more details and interpretation of the results with regard to the potential use of the intended dosimeter. To that end, a procedure on how gelatin can be used, and the values of radiation read with precision and accuracy for the materials under study will be reported.

4. Conclusion

Halal gelatins from camel, bovine, and fish bones were successfully extracted by using chemical pretreatment and heating methods. The preliminary findings demonstrated that the use of AgNPs embedded in gelatin caused the enhancement of the optical absorption spectrum and X-ray radiation absorption as an Ag colloidal nanoparticle solution is added to gelatin solution in elaborated samples. Bovine gelatin/AgNPs demonstrated the highest X-ray absorption, followed by camel and fish gelatin. The preliminary results show that the free-standing film-based gelatin/AgNPs produced can be recommended as a reliable material for making radiation dosimetry devices for low-energy external radiotherapy sources. However, more research is required to fully investigate the potential radiation applications of camel, fish, and bovine bone-extracted gelatin, as well as to determine its effectiveness and safety in these applications.

Acknowledgements

The authors extend their appreciation to the Deanship of Research and Graduate Studies at University of Tabuk for funding this work through Research no. S-1444-0157

References

[1] Macchione MA, Lechón Páez S, Strumia MC, Valente M, Mattea F. Chemical overview of gel dosimetry systems: a comprehensive review. *Gels.* 2022;8(10): 663.

[2] Azadeh P, Amiri S, Mostaar A, Joybari AY, Paydar R. Evaluation of MAGIC-f polymer gel dosimeter for dose profile measurement in small fields and stereotactic irradiation. *Radiat Phys Chem.* 2022;194:109991.

[3] Kron T, Metcalfe P, Pope JM. Investigation of the tissue equivalence of gels used for NMR dosimetry. *Phys Med Biol.* 1993;38:139–50.

[4] Al-Kahtani HA, Jaswir I, Ismail EA, Ahmed MA, Monsur Hammed A, Olorunnisola S, Octavianti F. Structural characteristics of camel-bone gelatin by demineralization and extraction. *Int J Food Prop*. 2017;20:11.

[5] Al-Hassan AA, Abdel-Salam AM, Al Nasiri F, Mousa HM, Nafchi AMM. *J Food Meas Charact.* 2021;15:4542–51.

[6] Ahmed MA, Al-Kahtani HA, Jaswir I, AbuTarboush H, Ismail EA. Extraction and characterization of gelatin from camel skin (potential halal gelatin) and production of gelatin nanoparticles. *Saudi J Biol Sci*. 2020;27(6):1596–601.

[7] Chan MF, Ayyangar K. Verification of water equivalence of FeMRI gel using Monte Carlo simulation. *Med Phys*. 1995;22(4):475–8.

[8] Keall P, Baldock C. A theoretical study of the radiological properties and water equivalence of Fricke and polymer gels used for radiation dosimetry. *Australas Phys Eng.Sci Med*. 1999;22:85–91.

[9] Schreiner LJ. Review of Fricke cel dosimeters. *J Phys Conf Ser.* 2004;3:9–21.

[10] De Deene Y, Hurley C, Venning A, Vergote K, Mather M, Healy B, et al. A basic study of some normoxic polymer gel dosimeters. *Phys Med Biol.* 2002;47(19):3441–63.

[11] Gustavsson H, Bäck SÅJ, Medin J, Grusell E, Olsson LE. Linear energy transfer dependence of a normoxic polymer gel dosimeter investigated using proton beam absorbed dose measurements. *Phys Med Biol*. 2004;49(17):3847–55.

[12] De Deene Y. Radiation dosimetry by use of radiosensitive hydrogels and polymers: mechanisms, state-of-the-art and perspective from 3D to 4D. *Gels.* 2022;8:599.

[13] Zhang P, Jiang L, Chen H, Hu L. Recent advances in hydrogel-based sensors responding to ionizing radiation. *Gels.* 2022;8:238.

[14] Nezhad ZA, Geraily G. A review study on application of gel dosimeters in low energy radiation dosimetry. *Appl Radiat Isot.* 2022;179:110015.

[15] Gayol G, Malano F, Montenovo CR, Pérez P, Valente M. Dosimetry effects due to the presence of Fe nanoparticles for potential combination of hyperthermic cancer treatment with MRI-based image-guided radiotherapy. *Int J Molec Sci*. 2023;24(1):514.

[16] Soliman YS, Tadros SM, Beshir WB, Saad GR, Gallo S, Ali LI, Naoum MM. Study of Ag nanoparticles in a polyacrylamide hydrogel dosimeters by optical technique. *Gels* 2022;.8(4):222.

[17] Sofi MA, Sunitha S, Sofi MA, Khadheer Pasha SK, Choi D. An overview of antimicrobial and anticancer potential of silver nanoparticles. *J King Saud Univ – Sci.* 2022;34(2): 101791.

[18] Kortov V. Materials for thermoluminescent dosimetry: current status and future trends. *Radiat Meas*. 2007;42:576–81.

[19] Kron T. Thermoluminescence dosimetry and its applications in medicine–Part 1: physics, materials and equipment. Australas *Phys Eng Sci Med*. 1994;17:175–99.

[20] Kry SF, Alvarez P, Cygler JE, DeWerd LA, Howell RM, Meeks S, et al. AAPM TG 191: clinical use of luminescent dosimeters: TLDs and OSLDs. *Med Phys.* 2020;47:e19–e51.

[21] Lye J, Dunn L, Kenny J, Lehmann J, Kron T, Oliver C, et al. Remote auditing of radiotherapy facilities using optically stimulated luminescence dosimeters. *Med Phys*. 2014;41:032102.

[22] Poirier Y, Kuznetsova S, Villarreal-Barajas JE. Characterization of nanodot optically stimulated luminescence detectors and high-sensitivity MCP-N thermoluminescent detectors in the 40–300 kVp energy range. *Med Phys*. 2018;45:402–13.

[23] Damulira E, Yusoff MNS, Omar AF, Mohd Taib NH. A review: photonic devices used for dosimetry in medical radiation. *Sensors.* 2010;19:2226.

[24] Inoue K, Yamaguchi I, Natsuhori M. Low-dose radiation effects on animals and ecosystems. In: Fukumoto M, editor. Preliminary study on electron spin resonance dosimetry using affected cattle teeth due to the Fukushima Daiichi nuclear power plant accident. Singapore: Springer, 2020.

[25] Kinoshita A, Baffa O, Mascarenhas S. Electron spin resonance (ESR) dose measurement in bone of Hiroshima A-bomb victim. *PLoS ONE* 2018;13:e0192444.

[26] Klein JS, Sun C, Pratx G. Radioluminescence in biomedicine: physics, applications, and models. *Phys Med Biol.* 2019;64:04TR01.

[27] Petisiwaveth P, Wanotayan R, Damrongkijudom N, Ninlaphruk S, Kladsomboon, S. Dosimetric performance of poly(vinyl alcohol)/silver nanoparticles hybrid nanomaterials for colorimetric sensing of gamma radiation. *Nanomaterials* 2022;12(7):1088.

[28] Titus D, Samuel EJJ, Srinivasan K, Roopan SM, Madhu CS. Silver nitrate-based gel dosimeter. *J Phys*: Conference Series. 847 012066.

[29] Vedelago J, Mattea F, Valente M. Integration of Fricke gel dosimetry with Ag nanoparticles for experimental dose enhancement determination in theranostics, *Appl Radiat Isot.* 2018;141:182–6.

[30] Badi N, Mekala R, Khasim S, Roy AS, Ignatiev A. Enhanced dielectric performance in PVDF/Al-Al_2O_3 core-shell nanocomposites. *J Mater Sci: Mater Electron.* 2018;29:10593–9.

[31] Wong C. Polymers for electronic and photonic application. Amsterdam: Elsevier; 2013.

[32] Nafee SS, Hamdalla TA, Shaheen SA. FTIR and optical properties for irradiated PVA–GdCl3 and its possible use in dosimetry. Phase Transit. 2017;90:439.

[33] Rashad M, Hanafy TA, Issa SAM. Structural, electrical and radiation shielding properties of polyvinyl alcohol doped with different nanoparticles. *J Mater Sci—Mater Electron.* 2020;31:15192.

[34] Al Misned G, Akman F, AbuShanab WS, Tekin HO, Kaçal MR, Issa SAM, et al. Novel Cu/Zn reinforced polymer composites: experimental characterization for radiation protection efficiency (RPE) and shielding properties for alpha, proton, neutron, and gamma radiations. *Polymers*. 2021;13:3157.

[35] Abdalsalam AH, Sakar E, Kaky KM, Mhareb MHA, Sakar BC, Sayyed MI, Gürol A. Investigation of gamma ray attenuation features of bismuth oxide nano powder reinforced high-density polyethylene matrix composites. *Radiat Phys Chem*. 2020;168:108537.

[36] Akman F, Kaçal MR, Almousa N, Sayyed MI, Polat H. Gamma-ray attenuation parameters for polymer composites reinforced with $BaTiO_3$ and $CaWO_4$ compounds. *Prog Nucl Energy*. 2020;121:103257.

[37] Hamdalla TA, Nafee SS. Bragg wavelength shift for irradiated polymer fiber Bragg grating. *Opt Laser Technol*. 2017;74:167.

[38] Pai S, Das IJ, Dempsey JF, Lam KL, Losasso TJ, Olch AJ, et al. TG-69: radiographic film for megavoltage beam dosimetry. *Med Phys*. 2007;34:2228.

[39] Hassan N, Ahmad T, Zain NM, Awang SR. Identification of bovine, porcine and fish gelatin signatures using chemometrics fuzzy graph method. *Sci Rep*. 2021;11:9793.

[40] Hashim DM, Che Man YB, Norakasha R, Shuhaimi M, Salmah Y, Syahariza ZA. Potential use of Fourier transform infrared spectroscopy for differentiation of bovine and porcine gelatins. *Food Chem*. 2010;118(3):856–60.

[41] Zilhadia KF, Betha OS, Supandi S. Diferensiasi gelatin sapi dan gelatin babi pada gummy vitamin C nmenggunakan methode kombinasi spektroskopi Fourier transform infrared (FTIR) dan principal component analysis (PCA). *Pharm Sci Res*. 2018;5(2):90–6.

[42] Barth A. Infrared spectroscopy of proteins. *Biochim Biophys Acta* (BBA)-*Bioenerg*. 2007;1767:1073–101.

[43] Al-Hassan AA, Abdel-Salam A.M, Al Nasiri F, Mousa HM, Nafch AM. Extraction and characterization of gelatin developed from camel bones. *J Food Meas Charact.* 2021;15:4542–51.

[44] Al-Kahtani HA, Jaswir I, Ismail EA, Ahmed MA, Hammed AM, Olorunnisola S, Octavianti F. Structural characteristics of camel-bone gelatin by demineralization and extraction. *Int J Food Prop*. 2017;20:2559–68.

[45] Fawale OS, Abuibaid A, Hamed F, Kittiphattanabawon P, Maqsood S. Molecular, structural, and rheological characterization of camel skin gelatin extracted using different pretreatment conditions. *Foods*. 2021;10: 1563.

[46] Kong J, Yu S. Fourier transform infrared spectroscopic analysis of protein secondary structures. *Acta Biochim Biophys Sin*. 2007;39:549–59.

[47] Nur Hanani ZA, Roos YH, Kerry JP. Fourier transform infrared (FTIR) spectroscopic analysis of biodegradable gelatin films immersed in water. *Int Congr Eng Food, Proc*. 2011.

[48] Alim-Al-Razy M, Bayazid GMA, Rahman RU, Bosu R, Shamma SS. Silver nanoparticle synthesis, UV-Vis spectroscopy to find particle size and measure resistance of colloidal solution. *J Phys*. 2020;1706:012020.

[49] Fuliful F, Hashim A, Madlool R. Calculating the X-ray attenuation coefficients of gelatin as human tissue substitute. *Austral J Basic Appl Sci*. 2017;11:21.

Received 2023-11-18
Accepted 2024-02-16